

Solubility of carbon in tetragonal ferrite in equilibrium with austenite

Jae Hoon Jang^a H. K. D. H. Bhadeshia^{a,b} Dong-Woo Suh^a

^a*Graduate Institute of Ferrous Technology, Pohang University of Science and Technology, Pohang 790-784, Republic of Korea*

^b*Materials Science and Metallurgy, University of Cambridge, U.K.*

Abstract

There are precise observations which indicate the reluctance of excess carbon within bainite or martensite to partition into adjacent austenite in spite of prolonged heat treatment at temperatures where carbon is mobile. To explain this, we report the first calculations of the solubility of carbon in tetragonal ferrite that is in equilibrium with austenite. It is found that the solubility is dramatically increased relative to the cubic form of ferrite, and the implications of this are discussed briefly.

Key words: solubility of carbon, martensite, bainite, quench and partitioning, ferrite, diffusion

It is known that when martensite in steels forms at temperatures below that for Zener ordering [1], it adopts a body-centred tetragonal crystal structure with carbon atoms located at one of the three sub-lattices of octahedral interstices. The lattice parameter ratio c/a depends on the carbon concentration according to the relationship $c/a = 1 + 0.045x_w$ where x_w is the concentration of carbon in wt% [2,3]. Whereas the equilibrium between ferrite and austenite in Fe-C is well established, that of austenite with tetragonal martensite has never been investigated. Why is this important?

There is new development in steel technology which uses a heat-treatment known colloquially as “quench and partitioning” in which a partially martensitic sample is heated momentarily to allow excess carbon to partition into the austenite and stabilise it to ambient temperature [4]. There are theoretical treatments of similar phenomena [5] which probe the partitioning of carbon from martensite into the residual austenite.

There are intriguing observations that carbon inherited by bainitic ferrite is reluctant to partition into the residual austenite in spite of prolonged heat

treatment [6–10]. Although early interpretations of this relied on carbon being trapped at dislocations, recent work has shown with clarity that large quantities of excess carbon remain in a defect-free solid solution [11,12].

In this discussion, the adjective *excess* implies a greater concentration than the solubility of carbon in α -ferrite which is in equilibrium with γ -austenite. The maximum solubility is a little greater than 0.02 wt% at a temperature of about 600 °C due to the retrograde shape of the $\alpha/\alpha + \gamma$ phase boundary [13,14]. These data therefore apply to cubic ferrite, and the circumstances could be different for the tetragonal version, with consequential implications on the interpretation of the phenomena described above.

We report, therefore, calculations of the solubility of carbon in tetragonal ferrite which is in equilibrium with austenite.

A $2 \times 2 \times 2$ supercell of the conventional body-centred cubic ferrite unit cell, which contains 16 Fe atoms, for the ferromagnetic state, was used for the first principles calculations. Carbon was permitted to locate both at octahedral and tetrahedral interstices, Fig. 1. The Kohn-Sham equation was solved self-consistently in terms of the total energy all-electron full-potential linearised augmented plane-wave method [15,16]. The exchange-correlation potential was according to the generalised gradient approximation scheme [17]. The integrations over the three dimensional Brillouin zone were performed by the tetrahedron method [18] over a $6 \times 6 \times 6$ Monkhorst-Pack mesh [19]. The degree of precision was defined by a plane-wave cutoff up to 21 Ry. The wave functions, the charge densities, and the potential were expanded with $l < 8$ lattice harmonics inside each muffin-tin sphere with the radius of 1.80 and 0.90 a.u. for the Fe and C atoms, respectively.

The density and potential were depicted by using a star-function cutoff at 340 Ry. Core electrons were treated fully relativistically, while valence states were calculated scalar relativistically, without considering spin-orbit coupling [20]. Self-consistency was assumed when the root-mean-square distances between the input and output total charges and spin densities were less than 1.0×10^{-4} electrons/a.u.³ The internal atomic positions are relaxed by using the total energy and force minimisation scheme using the Broyden method to find the multidimensional zero [21]. The structure was said to be relaxed when the force on each atom < 1 mRy/a.u., and when the position did not change more than 3×10^{-3} a.u.

Fig. 2 shows calculations of the carbon dissolution energies, based on graphite and body-centred cubic (BCC) ferrite as the reference states. The referenced carbon is assumed to be graphite and its values are obtained from the diamond structure with a correction of 17 meV [22]. The concentration of carbon in Fe-C is set to 1/17 mole fraction, which corresponds to about 1.3 wt%. The

dissolution energies were calculated based on the following equation.

$$\Delta H_s = \frac{E(\text{Fe}_{16}\text{C}_1) - 16 \times E(\text{Fe}) - E(\text{C})}{17} \quad (1)$$

where ΔH_s represents an enthalpy change referred to as the ‘dissolution energy’ and E the appropriate energy. Table 1 lists the equilibrium atomic volumes, solution enthalpies of carbon and nearest atomic distance between Fe and C in ferromagnetic BCC Fe at 0 K for both the unrelaxed and relaxed structures. The equilibrium atomic volume of pure ferrite is calculated to be 11.54 \AA^3 . The dissolution of carbon expands this to 13.15 and 12.93 \AA^3 , which are about 14% and 12% larger, for unrelaxed octahedral and tetrahedral sites, respectively. The dissolution energies for unrelaxed tetrahedral and octahedral site are $24.89 \text{ kJ mol}^{-1}$ and $20.19 \text{ kJ mol}^{-1}$, respectively.

Since the tetrahedral site has a larger interstitial radius in the hard sphere model, the dissolution energy for the tetrahedral site is smaller compared with that for the octahedral interstice. However, the dissolution energies changed after atomic position relaxation, to 3.77 kJ mol^{-1} and 8.49 kJ mol^{-1} for the octahedral and tetrahedral sites. These results are entirely expected because the octahedral interstice in ferrite is markedly irregular, so that the main deformation due to the location of carbon occurs along one of the axes parallel to $[100]_\alpha$, whereas the iron atoms along the other two orthogonal axes (parallel to $\langle 011 \rangle_\alpha$) are located much further apart. In contrast, all principal directions of the tetrahedral interstice are expanded. Diffusion experiments indicate that much less than 10^{-3} of available carbon atoms reside in the tetrahedral interstices [23]; continuum strain energy calculations [24] also show the octahedral interstices as the preferred sites for carbon to be located.

Fig. 3 shows the calculated dissolution energies of carbon in ferrite at octahedral interstices with different degrees of unit-cell tetragonality, as a function of atomic volume for the fully relaxed structure. Interestingly, there is an optimum lattice parameter ratio c/a for least dissolution energy. For $c/a = 1.00$, the dissolution energies is $\Delta H_s^\alpha = 3.77 \text{ kJ mol}^{-1}$ and decreases systematically until a ratio of 1.07 is achieved, with $\Delta H_s^{\alpha'} = 2.76 \text{ kJ mol}^{-1}$, after which it increases. This may be understood by the fact that the interference between the iron and carbon atoms increases with c/a along the two $\langle 011 \rangle$ directions which have a third greater elastic modulus when compared with the $[100]$ orientation. There must therefore exist an optimum c/a ratio, and the ratio of 1.07 compares well with the value of 1.06 obtained from the experimental equation of Honda and Nishiyama [2,3] for 1.3 wt% carbon.

Some comments on the magnitudes of the dissolution energies are appropriate. The dissolution energies of carbon in ferrite are about 6.24 kJ mol^{-1} in TCFE6 ThermoCalc database [25], while the first principles calculations indicate 3.77 kJ mol^{-1} whereas those reported using a pseudo-potential scheme

give 3.29 kJ mol^{-1} [26]. Relative to the data in TCFE6, the calculations reported here are for a large carbon concentration (16Fe-1C) so the smaller dissolution energy may be attributed to the difference of atomic volume. The volume per atom is much smaller for pure iron; a smaller value leads to a higher dissolution energy (Fig. 2) so the 6.24 kJ mol^{-1} of TCFE6 is reasonable for very low carbon ferrite.

The calculated dissolution energies for the body-centred tetragonal structure were introduced into the standard thermodynamic databases and the equilibrium with austenite was calculated between 0 to 1000°C . The results are presented in Fig 4 for the case where $c/a = 1.07$, which would be the tetragonality expected if austenite with a carbon concentration of 1.3 wt% transformed into martensite; such a concentration is typical of the carbon concentration of retained austenite in many alloy systems used commercially. The difference of dissolution energies of the BCC and tetragonal structure, $\Delta G^{\alpha\alpha'} = H_s^{\alpha'} - H_s^\alpha$, is $-1.01 \text{ kJ mol}^{-1}$, according to the first principles calculations. Fig. 4 shows the binary phase diagram of Fe-C system allowing body-centred tetragonal cubic structure and FCC phases to coexist with a reduced dissolution energy in the BCT structure relative to BCC. It is evident that the solubility of carbon in the BCT phase in equilibrium with austenite is much greater than for BCC ferrite. It is noteworthy that the maximum in solubility arises at a temperature of about 400°C which is often the temperature corresponding to the quench and partitioning heat-treatment [27].

In summary, first-principles calculations suggest that when tetragonal ferrite is in equilibrium with austenite, it has a much greater solubility for carbon than is the case for cubic ferrite in the same circumstances. The primary reason for this is the fact that the octahedral interstice is irregular and an increase in tetragonality enhances the fit of the carbon atom with respect to the iron atoms parallel to the shortest axis along [100], until a point is reached where the c/a ratio becomes so large that the fit along the stiffer $\langle 011 \rangle$ directions becomes limiting. The essential conclusion is that once the ferrite acquires tetragonality, it becomes easier for it to retain excess carbon.

It is possible that the present calculations may explain the observed reluctance for the “excess” carbon present in bainitic ferrite to partition into the residual austenite despite prolonged heat treatment, and a consideration of tetragonality might form a better basis for a variety of kinetic theories on industrially important processes. The tetragonality may exist over a long range, but the possibility of a domain structure such as that found in minerals which undergo cubic to tetragonal transitions, should not be ruled out.

The $\alpha/\alpha + \gamma$ equilibrium phase boundary has a retrograde shape (Fig. 4b) whether ferrite is BCC [13,14] or BCT as proven here. The fraction of ferrite should therefore go through a maximum as a function of temperature. How-

ever, this applies to two-phase $\alpha + \gamma$ equilibrium. If cementite precipitates in contact with ferrite, as in the quench and partitioning process, then the $\alpha/\alpha + \text{Fe}_3\text{C}$ phase boundary is not retrograde so the fraction of α increases monotonically as the temperature is reduced. With carbide-free bainite, reversibility is compromised by the plastic relaxation of the shape deformation and some partitioning of carbon. This is the reason why shape memory effects are not observed in low-alloy steels.

This work was supported by the Steel Innovation Programme by POSCO and the World Class University programme (Project No. R32-2008-000-10147-0) by the National Research Foundation of Korea.

References

- [1] J. C. Fisher, J. H. Hollomon, D. Turnbull: *Metals Trans.* 185 (1949) 691.
- [2] E. Honda, Z. Nishiyama: *Sci. Rep. of Tohoku Imperial Uni.* 21 (1932) 299.
- [3] J. W. Christian: *Mat. Trans., JIM* 33 (1992) 208.
- [4] J. Speer, D. K. Matlock, B. C. D. Cooman, J. G. Schroth: *Acta Mat* 51 (2003) 2611.
- [5] H. K. D. H. Bhadeshia: *Met. Sci.* 17 (1983) 151.
- [6] H. K. D. H. Bhadeshia, A. R. Waugh: *Acta Metall.* 30 (1982) 775.
- [7] M. Peet, S. S. Babu, M. K. Miller, H. K. D. H. Bhadeshia: *Scr. Mat.* 50 (2004) 1277.
- [8] F. G. Caballero, M. K. Miller, S. S. Babu, C. Garcia-Mateo: *Acta Mat.* 55 (2007) 381.
- [9] C. Garcia-Mateo, M. Peet, F. G. Caballero, H. K. D. H. Bhadeshia: *Mat. Sci. Techn.* 20 (2004) 814.
- [10] F. G. Caballero, M. K. Miller, A. J. Clarke, C. Garcia-Mateo: *Scr. Mat.* 63 (2010) 442.
- [11] F. G. Caballero, M. K. Miller, C. Garcia-Mateo, J. Cornide: *J. Alloys Comp.* (2012) doi:10.1016/j.jallcom.2012.02.130.
- [12] F. G. Caballero, M. K. Miller, C. Garcia-Mateo, J. Cornide, M. J. Santofimia: *Scr. Mat.* (2012) 10.1016/j.scriptamat.2012.08.007.
- [13] H. I. Aaronson, H. A. Domian, G. M. Pound: *TMS-AIME* 236 (1966) 753.
- [14] H. K. D. H. Bhadeshia: *Met. Sci.* 16 (1982) 167.
- [15] E. Wimmer, H. Karkauer, M. Weinert, A. J. Freeman: *Phys. Rev. B* 24 (1981) 864.

- [16] M. Weinert, E. Wimmer, A. J. Freeman: Phys. Rev. B 26 (1982) 4571.
- [17] J. P. Perdew, K. Burke, M. Ernzerhof: Phys. Rev. Lett. 77 (1996) 3865.
- [18] J. Rath, A. J. Freeman: Phys. Rev. B 11 (1975) 2109.
- [19] H. J. Monkhorst, J. D. Pack: Phys. Rev. B 13 (1976) 3865.
- [20] D. D. Koelling, B. N. Harmon: J. of Phy. C 10 (1977) 3107.
- [21] W. Mannstadt, A. J. Freeman: Phys. Rev. B 55 (1997) 13298.
- [22] C. K. Ande, M. H. F. Sluiter: Acta Mat. 58 (2010) 6276.
- [23] R. B. McLellan, M. L. Rudee, T. Ishibachi: Trans. A.I.M.E. 233 (1965) 1939–1943.
- [24] D. N. Beshers: J. App. Phys. 36 (1965) 290–300.
- [25] J. Bratberg: TCFE6–TCS Steels/Fe–Alloys Database, Version 6.2: Tech. rep.: Thermo–Calc software AB: Stockholm, Sweden (2011).
- [26] D. E. Jiang, E. A. Carter: Phys. Rev. B 67 (2003) 214103.
- [27] J. G. Speer, D. V. Edmonds, F. C. Rizzo, D. K. Matlock: Curr. Opin. Sol. St. and Mat. Sci. 8 (2004) 219.

Table 1

Equilibrium atomic volume, dissolution energy of carbon (ΔH_s) and nearest atomic distance D between Fe and C in ferromagnetic BCC Fe at 0 K for both unrelaxed and relaxed structures.

ine	Atomic Volume / \AA^3		$\Delta H_s/\text{kJ mol}^{-1}$		$D_{\text{Fe-C}} / \text{\AA}$	
	unrelaxed	relaxed	unrelaxed	relaxed	unrelaxed	relaxed
ine Octahedral	13.15	12.43	24.89	3.77	1.459	1.763
Tetrahedral	12.93	12.32	20.19	8.49	1.627	1.815
ine						

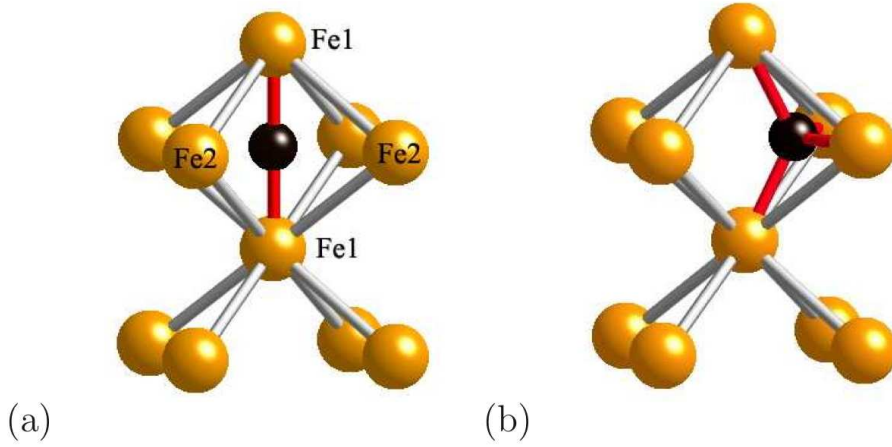
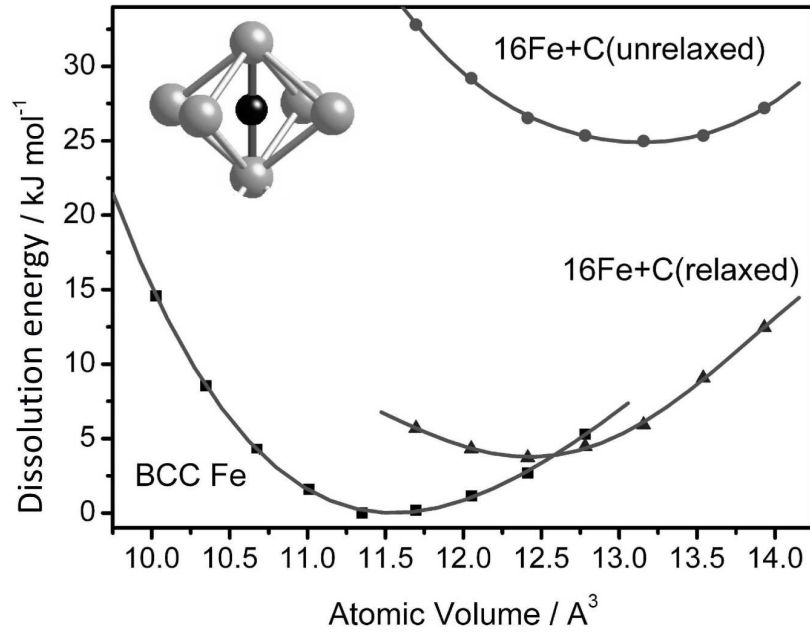
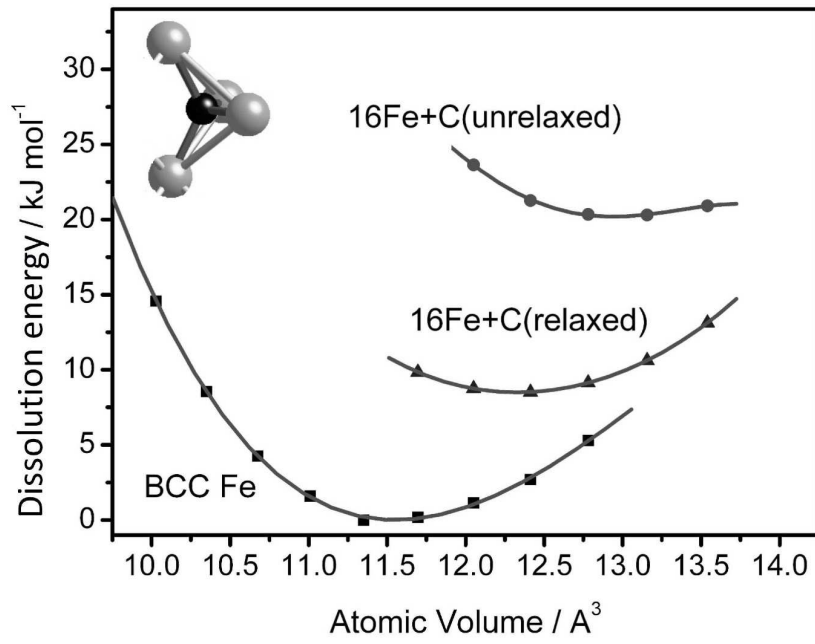


Fig. 1. The location of carbon in ferrite, at (a) octahedral interstice. The vertical axis of the octahedron is parallel to $[100]$ whereas the horizontal edges are parallel to $[011]$ and $[0\bar{1}1]$ directions. (b) Tetrahedral interstice.



(a)



(b)

Fig. 2. Calculated dissolution energies of carbon in ferrite at (a) octahedral and (b) tetrahedral sites, respectively, obtained from first principles calculations as a function of atomic volume.

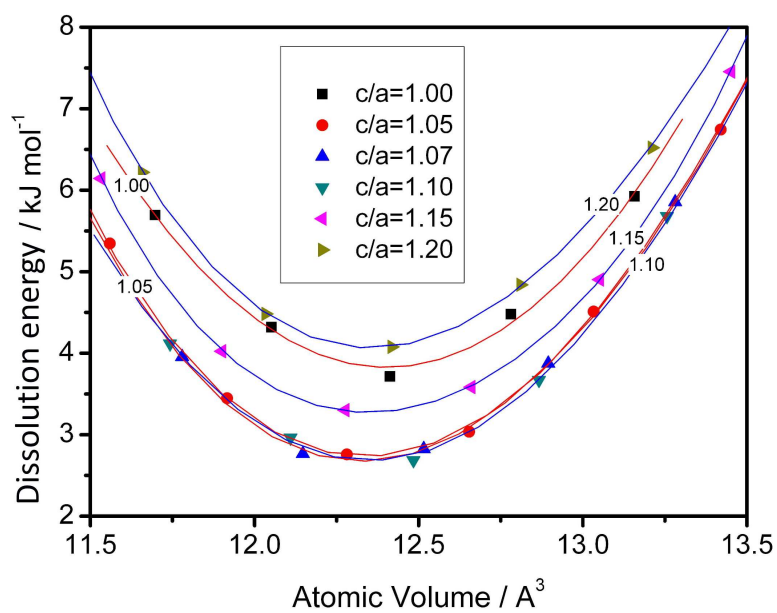
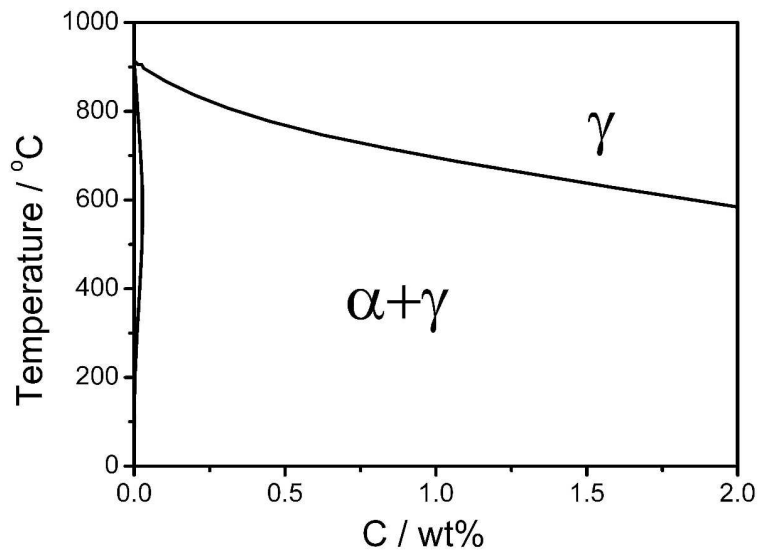
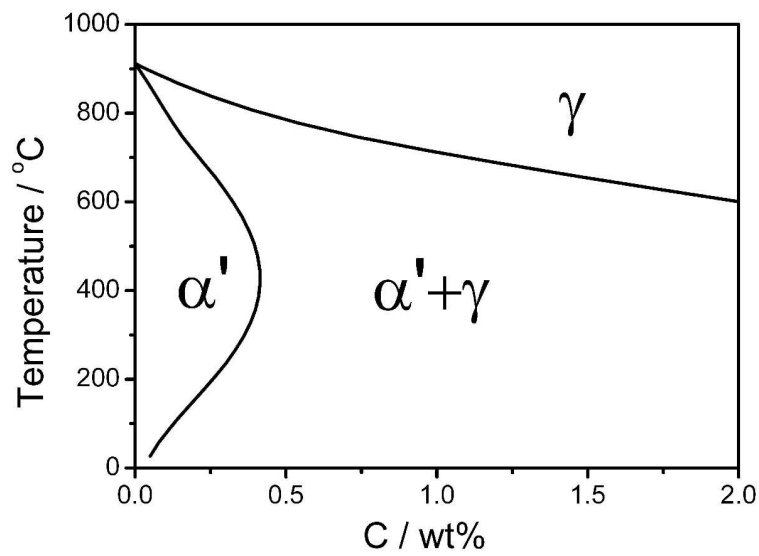


Fig. 3. Calculated dissolution energies of carbon in ferrite at octahedral sites with different tetragonality as a function of atomic volume obtained from first principles calculations.



(a)



(b)

Fig. 4. Binary phase diagram of Fe-C system allowing (a) BCC and FCC phases with TCFE6.2 database and (b) body centred tetragonal structure and FCC phases with $\Delta G^{\alpha'}(1/17 \text{ mole fraction}) = -1.01 \text{ kJ mol}^{-1}$, respectively